International Journal of Recent Technology and Engineering (IJRTE)
ISSN: 2277-3878 (Online), Volume-8, Issue-1, May 2019

The Structural and Electrical Properties of Flexible $PMMA_{IL}$/LiTf Films

Nabilah Akemal Muhd Zailani, Famiza Abdul Latif, Abdul Malik Marwan Ali, Mohd Azri Ab Rani, Muhd Zu Azhan Yahya

Abstract*: To date, poly (methyl methacrylate) (PMMA) in film form, exhibited the most mechanical stability towards lithium electrode. Unfortunately, commercial PMMAs even at high molecular weight were not able to produce flexible film. This is due to the presence of oxygen atoms that incline to form interchain crosslinking via hydrogen bonding. Therefore, the opportunity of the PMMA chains to form hydrogen bonding was hindered by encapsulating 1-methyl-3-pentamethyldisiloxymethylimidazolium bis(trifluoromethylsulfonyl)imide, $[(SiOSi)C_1C_1im][NTf_2]$ during free radical polymerization of MMA. It was found that, this newly synthesized PMMA containing IL ($PMMA_{IL}$) produced flexible and transparent films with ionic conductivity of ~10^{-7} S cm^{-1}. Though the ionic conductivity obtained is comparable with other doped PMMA film electrolytes that had been studied, it is still considered as low for application in energy storage devices. Thus, in this study, the conductivity of the $PMMA_{IL}$ was further enhanced by the addition of lithium triflate (LiTf) using solvent casting technique. The highest ionic conductivity for this doped $PMMA_{IL}$ achieved ~10^{-4} S cm^{-1} which fits the minimum requirement for energy storage devices. As confirmed from Fourier Transform Infrared spectroscopy (FTIR) and Optical Microscope (OM) analyses, the increase in ionic conductivity was due to the suppression of the semicrystalline structure of $PMMA_{IL}$ owing to the added salt.

***Index Terms*: Ionic liquid, Lithium triflate, PMMA, Polymer electrolytes.**

I. INTRODUCTION

To date, film type PMMA electrolytes have been extensively modified by adding plasticizers [1] or organic fillers [2] or blending it with other polymers with lower T_g [3]. All these initiatives are to improve its brittleness [3] that caused poor contact with the electrode. This in turn, creates air gap between the electrolyte film and the electrode that becomes additional resistance for the ionic conduction. Unfortunately, these efforts have shown drawbacks such as formation of agglomerates due to excessive addition of fillers, phase separation due to incompatibility of PMMA with certain polymer during the blending or the mechanical properties of the film became worsen when certain amount of plasticizer was added.

Recently, the addition of ionic liquids, (IL) such as 1-butyl-3-methylimidazolium bis(trifluoromethylsulfonyl) imide [4], 1-butyl-3-methylimidazolium tetrachloroferrate [5] etc. have slightly improved the brittleness of the PMMA film. However, the ionic conductivity achieved is still below the minimum requirement for application in any energy storage devices [6]. Therefore, in this study, a new PMMA that has been synthesized by encapsulating $[(SiOSi)C_1C_1im][NTf_2]$ ionic liquid into the polymer matrix during free radical polymerization of MMA ($PMMA_{IL}$) was used as the main polymer host. This $PMMA_{IL}$ alone has exhibited the ionic conductivity of ~10^{-7} S cm^{-1} [7] which is comparable with other doped PMMA electrolyte films [8]-[9]. The ionic conductivity of this $PMMA_{IL}$ will be further enhanced by the addition of LiTf as the additional conducting species.

II. METHODOLOGY

A. Synthesis of bulk $PMMA_{IL}$

The synthesis of bulk $PMMA_{IL}$ via free radical polymerization of MMA in IL of $[(SiOSi)C_1C_1im][NTf_2]$ was carried out as previously mentioned [7].

B. Preparation of films

The bulk $PMMA_{IL}$ was then made into films by solvent casting technique [8].The $PMMA_{IL}$ with wt% composition of MMA: IL (70:30) was chosen to be doped with LiTf due to its high ionic conductivity and amorphosity if compared to the other compositions [7]. To obtain the salt doped $PMMA_{IL}$ films, the solvent casting technique was applied with fixed amount of bulk $PMMA_{IL}$ (0.3 g) and varied amount of salt (0-50 wt% LiTf). These films were then labelled as $PMMA_{IL}$, D5-$PMMA_{IL}$, D10-$PMMA_{IL}$, D20-$PMMA_{IL}$, D30-$PMMA_{IL}$, D40-$PMMA_{IL}$ and D50-$PMMA_{IL}$ respectively.

C. Characterization techniques

The FTIR spectra were recorded in the absorbance mode over a frequency range of 4000-600 cm^{-1} with 2 cm^{-1} resolution using Thermo Fisher Scientific Nicolet iS 10 equipped with Attenuated Total Reflectance (ATR). Nikon ECLIPSE ME 600 optical microscope was used to observe the morphology of the films.

Revised Manuscript Received on 30 May 2019.
***** Correspondence Author
Nabilah Akemal Muhd Zailani*, Faculty of Applied Sciences, Universiti Teknologi MARA Shah Alam, Selangor, Malaysia.
Famiza Abdul Latif, Faculty of Applied Sciences, Universiti Teknologi MARA Shah Alam, Selangor, Malaysia.
Abdul Malik Marwan Ali, Faculty of Applied Sciences, Universiti Teknologi MARA Shah Alam, Selangor, Malaysia
. **Mohd Azri Ab Rani**, Faculty of Applied Sciences, Universiti Teknologi MARA Shah Alam, Selangor, Malaysia
Muhd Zu Azhan Yahya, Faculty of Defence Science & Technology, Universiti Pertahanan Nasional Malaysia, Kuala Lumpur, Malaysia.

© The Authors. Published by Blue Eyes Intelligence Engineering and Sciences Publication (BEIESP). This is an open access article under the CC-BY-NC-ND license http://creativecommons.org/licenses/by-nc-nd/4.0/

The impedance of the films were determined from the Cole-Cole plots obtained from HIOKI 3532-50 LCR Hi Tester analyzer from 100 Hz to 1 MHz at room temperature. From the Cole-cole plots, the bulk resistance (R_b) of the films were determined and hence the ionic conductivity (σ) of the films were calculated as the equation below [10].

$$\sigma = \frac{l}{R_b \cdot A} \quad (1)$$

where R_b is the bulk resistance (Ω), l is the sample thickness (cm) and A is the effective contact area of the electrode and the electrolyte (cm^2). From the impedance data, the dielectric constant (ε_r), dielectric loss (ε_i), real part of electrical modulus (M_r) and imaginary electric modulus (M_i) were obtained from the following equations [10].

$$\varepsilon_r = \frac{Z_i}{\omega \cdot C_0 (Z_r^2 + Z_i^2)} \quad (2)$$

$$\varepsilon_i = \frac{Z_r}{\omega \cdot C_0 (Z_r^2 + Z_i^2)} \quad (3)$$

$$M_r = \frac{\varepsilon_r}{(\varepsilon_r + \varepsilon_i)} \quad (4)$$

$$M_i = \frac{\varepsilon_i}{(\varepsilon_r + \varepsilon_i)} \quad (5)$$

where C_0 is equal to $\varepsilon_0 A/t$, ε_0 is the permittivity of the free space (8.85×10^{-14} F cm^{-1}) and ω is angular frequency ($\omega = 2\pi f$).

III. RESULTS AND DISCUSSIONS

A. Formation of films

Solid, transparent and free standing films of $PMMA_{IL}$ with improved flexibility were obtained when 5, 10, 20, 30 and 40 wt% of LiTf were added. Above these compositions (50 wt% LiTf) the film became sticky and difficult to be peeled off from the Teflon dish, thus, the sample was discarded and not further characterized.

B. Morphological Studies

As shown in Fig. 1, the added LiTf was observed to reside inside the grains of the $PMMA_{IL}$ causing the grain size to become bigger (Table 1). However, when ≥ 20 wt% of salt was added, the grains were no longer observed due to the suppression of the semicrystalline structure of the $PMMA_{IL}$ hence suggesting the formation of more amorphous phase of the system. On the other hand, the excess salt or undissociated salt was found to be clumping with addition of ≥ 20 wt% of LiTf and this phenomenon might be contributed by two factors. The first factor is probably due to the large molecule of IL that limits the number of LiTf salt that can be accommodated in the $PMMA_{IL}$ system. The second factor might be due to the low molecular weight of $PMMA_{IL}$ host (8.8×10^3 g mol^{-1}) [7] which only able to provide a limited number of coordinating sites hence preventing the chance for more ions to dissociate. At 40 wt% LiTf, the clumping of salt became excessive and a congested structure was formed.

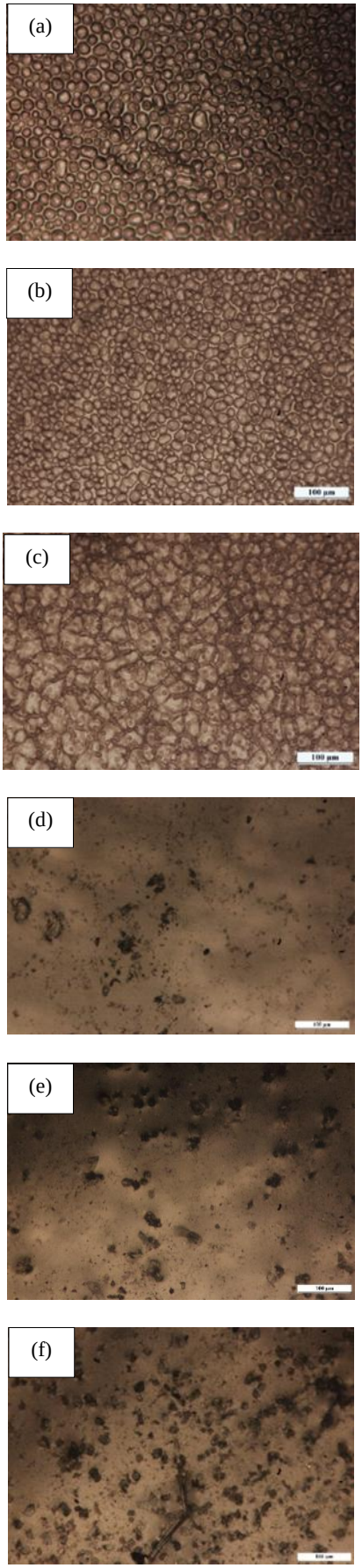

Fig. 1: Optical micrographs for Dx-$PMMA_{IL}$ system (a) $PMMA_{IL}$ (b) D5-$PMMA_{IL}$ (c) D10-$PMMA_{IL}$ (d) D20-$PMMA_{IL}$ (e) D30-$PMMA_{IL}$ and (f) D40-$PMMA_{IL}$

Table 1: Average grain size for D*x*-PMMA$_{IL}$

System	Average grain size (μm)
PMMA$_{IL}$	35
D5-PMMA$_{IL}$	38
D10-PMMA$_{IL}$	41

C. FTIR studies

Fig. 2 depicts the FTIR spectra of the D*x*-PMMA$_{IL}$ system. The C=O and -OCH$_3$ peaks of PMMA$_{IL}$ were observed at 1725 cm^{-1} and 1456 cm^{-1} respectively. The intensities of these peaks were reduced when LiTf salt was added indicating the formation of polymer-salt complex. The shifting of the wavenumber can be related to the strength of the interaction between the constituents in the polymer electrolytes based on equation below [11].

$$E = hv \tag{6}$$

where E equals to energy in Joules, h denotes to Planck's constant and v equals to wavenumber (cm^{-1}). As the energy (E) is directly proportional to the wavenumber (v), shifting to higher wavenumber indicates strong interaction and vice versa.

It was found that the C=O band shifted to lower wavenumber indicating that the interaction between the C=O and Li^+ ion of the salt is weaker than the interaction that occurred between the ion and the –OCH$_3$ group of the PMMA$_{IL}$ that caused the –OCH$_3$ band to shift to higher wavenumber. This was due to the occurrence of steric hindrances at C=O which gives difficulty for the Li^+ ions to be attached to it. This was supported by the study done by Sim *et al.* [12] which reported that the Li^+ ions prefer to form complexation with the C-O-*R* (*R*= CH_3, C_2H_5, etc.) of acrylates polymer due to the freedom of rotation for a single-bond if compared to the constrained rotation of the double bonded C-O group.

The C-H stretching, S-O stretching and C-F stretching peak intensities of IL in PMMA$_{IL}$ at 3152 cm^{-1}, 1351 cm^{-1} and 1051 cm^{-1} respectively were slightly reduced when LiTf salt was added hence confirming the interaction between the IL and salt. The upshift of the wavenumber for both C-H stretching (cation) and C-F stretching (anion) indicates the occurrence of strong interaction between IL and salt.

Upon addition of LiTf to the PMMA$_{IL}$, new peaks representing the triflate anions were observed at ~1030 cm^{-1} and ~1170 cm^{-1} which can be assigned to the SO_3 stretching and CF_3 stretching respectively. There is no changes in the wavenumber for CF_3 stretching and the slight increase in the wavenumber for SO_3 stretching was observed indicating the occurrence of weak interaction between PMMA$_{IL}$ and LiTf. There was no other new peak observed after the addition of LiTf hence proving that there is no chemical bond formed between PMMA$_{IL}$ and LiTf and the polymer-salt interaction only occurred via dative bond.

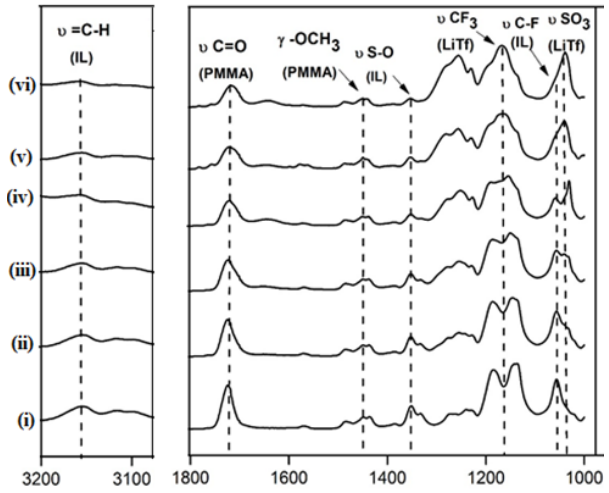

Fig. 2: FTIR Spectra for D*x*-PMMA$_{IL}$ system (i) PMMA$_{IL}$ (ii) D5-PMMA$_{IL}$ (iii) D10-PMMA$_{IL}$ (iv) D20-PMMA$_{IL}$ (v) D30-PMMA$_{IL}$ and (vi) D40-PMMA$_{IL}$

The vibrational mode of SO_3 can be used to classify between the free ions, ion pairs or undissociated ion and ion aggregates in the polymer-salt complex which appear in the region between 1030-1034 cm^{-1}, 1040-1045 cm^{-1} and 1049-1053 cm^{-1} respectively [12]. Fig. 3 shows the deconvolution of the FTIR spectra in the SO_3 stretching region for D*x*-PMMA$_{IL}$ system.

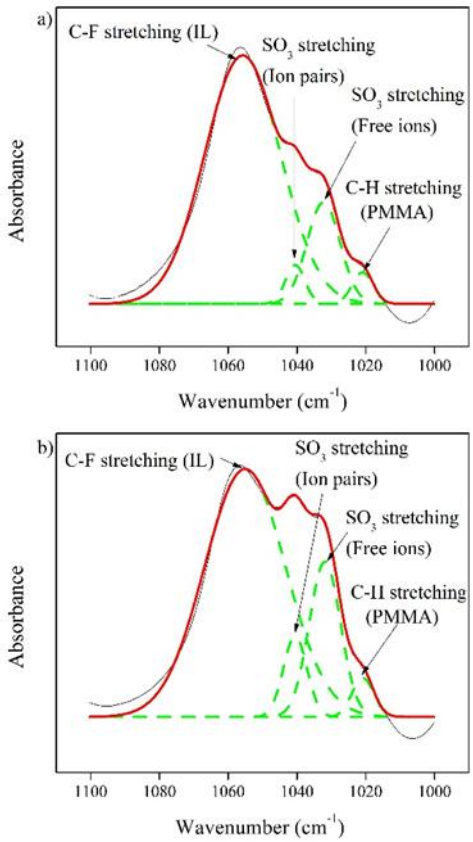

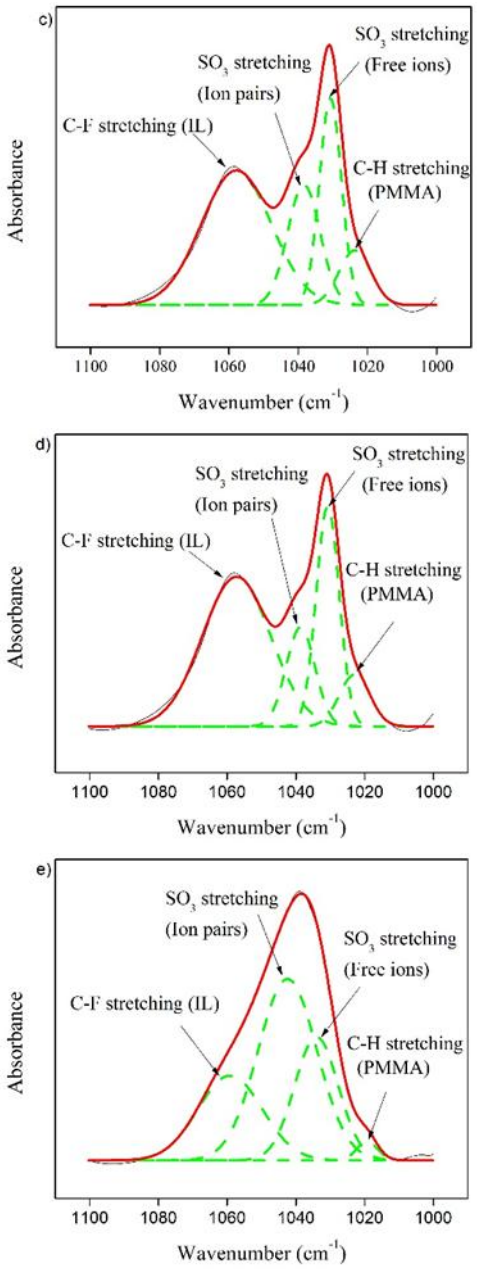

Fig. 3: Deconvolution and Band Fitting of FTIR spectra from 1100-1000 cm^{-1} for a) D5-$PMMA_{IL}$ b) D10-$PMMA_{IL}$ c) D20-$PMMA_{IL}$ d) D30-$PMMA_{IL}$ and e) D40-$PMMA_{IL}$

The band fitting shows the presence of the characteristic peak of PMMA (C-H stretching) at ~1020 cm^{-1}, C-F stretching of IL at ~1050 cm^{-1} and different ionic species of the SO_3 stretching at 1040-1030 cm^{-1} for all the samples. The SO_3 stretching peak observed at 1030-1032 cm^{-1} represents the free ions while the peak for ion pairs or undissociated ions was observed at 1038-1040 cm^{-1}. Interestingly, there are no peaks observed for ion aggregates even at highly congested sample (D40-$PMMA_{IL}$). This means that, the congestion structure observed for this sample is only due to presence of ion pairs or undissociated salt.

The number density (n), mobility (μ) and diffusion coefficient (D) of free ions for Dx-$PMMA_{IL}$ system were calculated using the equations below [13].

$$n = \frac{M \times N_A}{V_T} \times \%FI \quad (7)$$

$$\mu = \frac{\sigma}{ne} \quad (8)$$

$$D = \frac{\mu K_B T}{e} \quad (9)$$

where %FI refers to percentage of free ions obtained from FTIR deconvolution, M is the number of moles of LiTf, N_A is the Avogadro's constant (6.02×10^{23} mol^{-1}) and V_T is the total volume of components present in the sample. σ is the conductivity of the sample at 303 K and e is electron charge (1.60×10^{-19} C). K_B is the Boltzmann constant (1.38×10^{-23} J K^{-1}) and T is 303 K.

The number density (n), mobility (μ) and diffusion coefficient (D) of free ions for Dx-$PMMA_{IL}$ system show increasing trend up to the addition of 30 wt% of LiTf (Table 2). The doping of 40 wt% LiTf however shows reduced value of n, μ and D of free ions hence explaining the congested structure of the sample as observed in its OM analyses (Fig.1). As D30-$PMMA_{IL}$ exhibits the highest value of n, μ and D of free ions, thus it is expected to exhibit the highest conductivity value.

Table 2: The n, μ and D of free ions for Dx-$PMMA_{IL}$ system

System	Number density (n) ($\times 10^{22}$ cm^{-3})	Mobility (μ) ($\times 10^{-10}$ cm^2 V^{-1} s^{-1})	Diffusion coefficient (D) ($\times 10^{-12}$ cm^2 s^{-1})
D5-$PMMA_{IL}$	0.98	5.13	1.34
D10-$PMMA_{IL}$	1.00	5.34	1.40
D20-$PMMA_{IL}$	5.38	174	456
D30-$PMMA_{IL}$	8.64	192	501
D40-$PMMA_{IL}$	6.29	0.005	0.01

D. *Conductivity studies*

Fig.4 show the Cole-cole plots for Dx-$PMMA_{IL}$ system at ambient temperature. The plots for $PMMA_{IL}$ and D5-D30 $PMMA_{IL}$ exhibit depressed semicircle while half semicircle was observed for D40-$PMMA_{IL}$ at high frequencies indicating the migration of ion in the bulk system [14]. The appearance of spike was observed at lower frequencies region (except for D40-$PMMA_{IL}$) and this indicates the capacitance characteristic of the samples [15].

The conductivity for Dx-$PMMA_{IL}$ system were calculated based on (1) and tabulated in Table 3. The conductivity is observed to increase with increasing LiTf content up to 30 wt% and then decrease when 40 wt% of LiTf was added. Maximum conductivity of 2.65×10^{-4} S cm^{-1} was achieved when 30 wt% of LiTF was added into the system. The increase in the conductivity values up to 30 wt % of LiTf was due to the increase in the n, μ and D of free ions as confirmed from the deconvoluted FTIR analyses (Fig.3). Also, the increase in the conductivity can be explained by the suppression of the semicrystalline structure of $PMMA_{IL}$ with 20 wt% and above addition of salt as observed in their OM analyses (Fig.1).

The ionic conductivity drastically decreases when 40 wt% of LiTf was added and this can be related to its congested structure due to the presence of high amount of ion pairs/ undissociated ions hence limiting the n, μ and D of free ions as confirmed from its deconvoluted FTIR analyses (Fig.3).

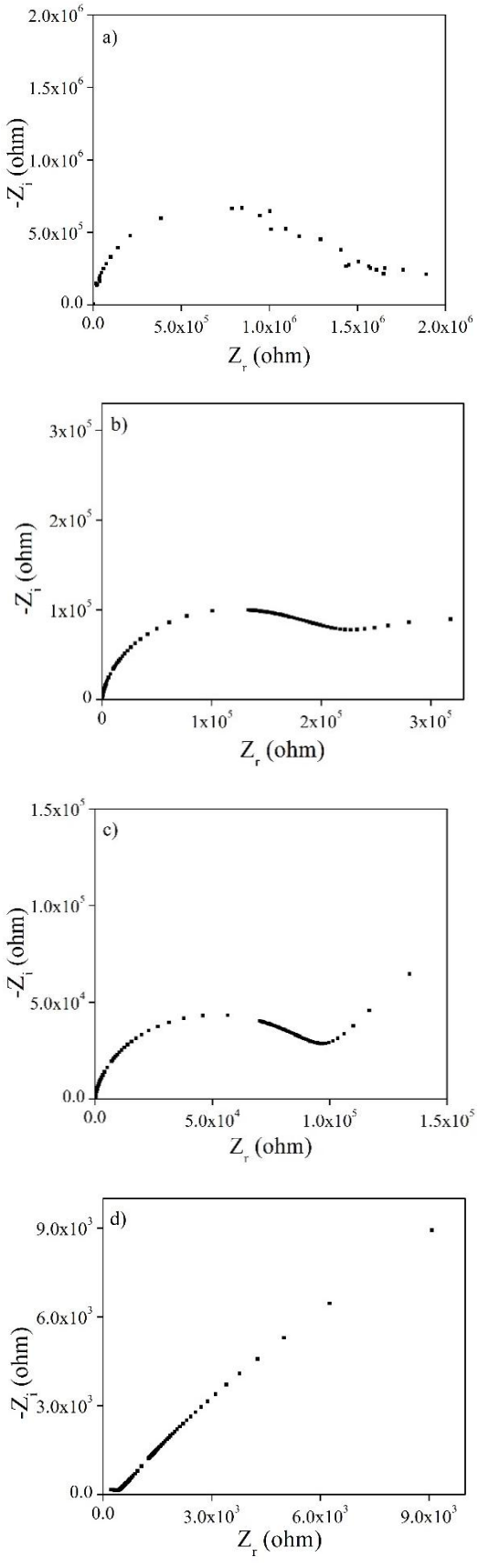

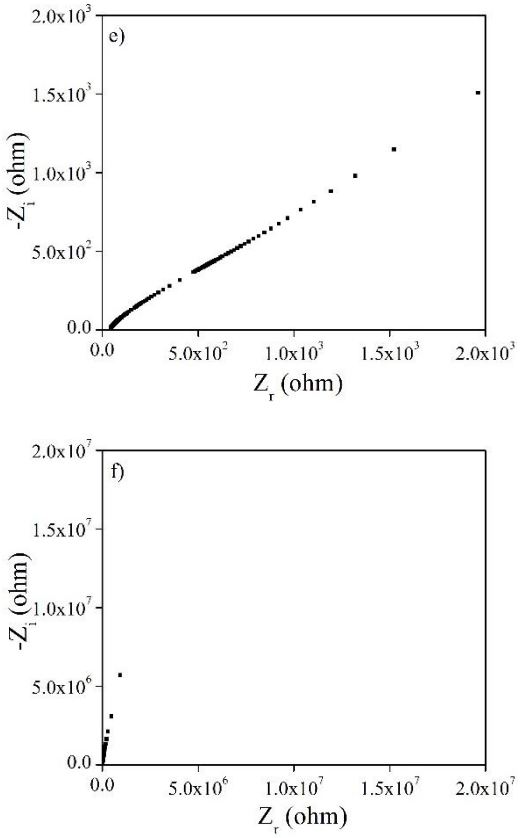

Fig. 4: Cole-cole Plots for a) $PMMA_{IL}$ b) D5-$PMMA_{IL}$ c) D10-$PMMA_{IL}$ d) D20-$PMMA_{IL}$ e) D30-$PMMA_{IL}$ and f) D40-$PMMA_{IL}$

Table 3: The Ionic Conductivity for Dx-$PMMA_{IL}$ System at Room Temperature

System	Ionic conductivity, σ (S cm^{-1}, 303 K)
$PMMA_{IL}$	1.72×10^{-7}
D5-$PMMA_{IL}$	8.57×10^{-7}
D10-$PMMA_{IL}$	8.12×10^{-7}
D20-$PMMA_{IL}$	1.50×10^{-4}
D30-$PMMA_{IL}$	2.65×10^{-4}
D40-$PMMA_{IL}$	5.27×10^{-9}

The dielectric studies were carried out in order to investigate the conductivity behaviour of the Dx-$PMMA_{IL}$ system based on composition dependence. Both the plots of ε_r and ε_i versus frequency were presented in Fig. 5 (a) and Fig. 5 (b) respectively. The rise of ε_r and ε_i at low frequency indicates that the electrode polarization and space charge effects have occurred. The polarization happened as the charges have enough time to accumulate at the interfaces before the electric field changes direction. At high frequency, the reversal rate of the electric field increase giving no time for the charges to accumulate at the interface resulting in low ε_r and ε_i [16].

Fig. 5 (c) and Fig. 5 (d) show the variation of the real (M_r) and imaginary (M_i) part of electrical modulus as a function of frequency respectively. At low frequencies region, M_r and M_i values tend to zero signifying that electrode polarization phenomena were almost negligible.

The appearances of relaxation peaks were detected in the M_i plots of the D5-$PMMA_{IL}$ and D10-$PMMA_{IL}$ compositions at high frequency region due to low ionic mobility contributed by their semicrystalline structure as observed in Fig. 1. There was no peak observed for addition of more than 10 wt% LiTf and the peak is expected to occur at higher frequencies, which confirm that the charges are mobile over longer distances [16] due to their high ionic mobility.

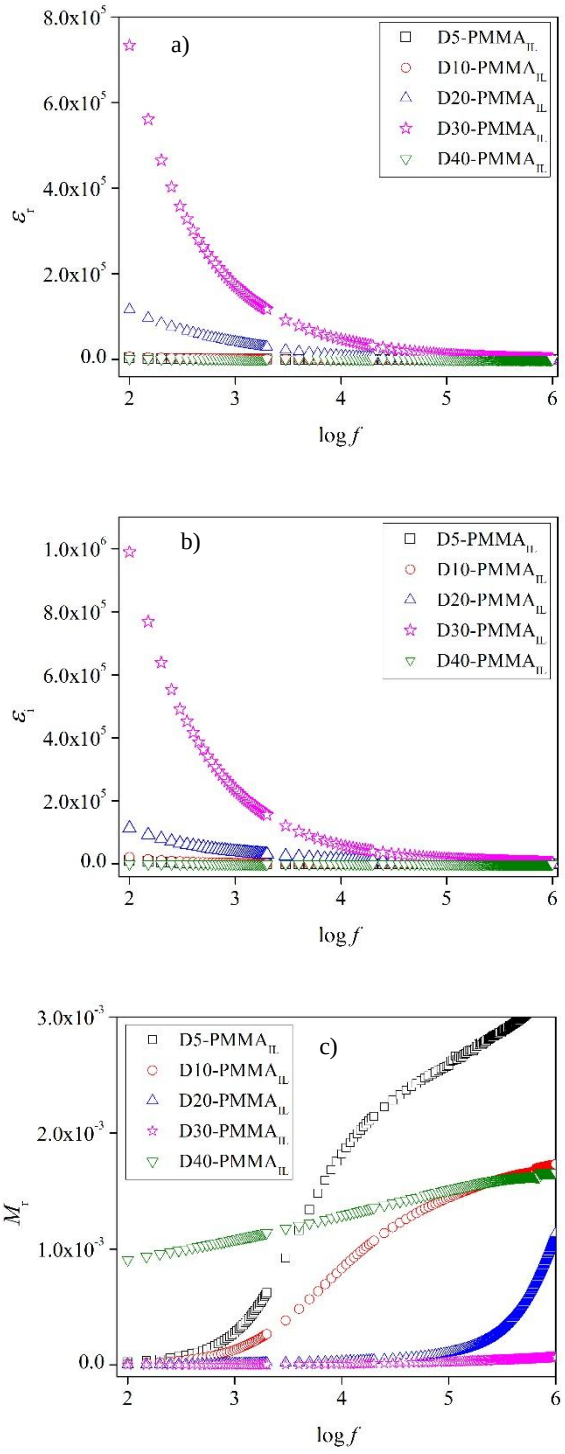

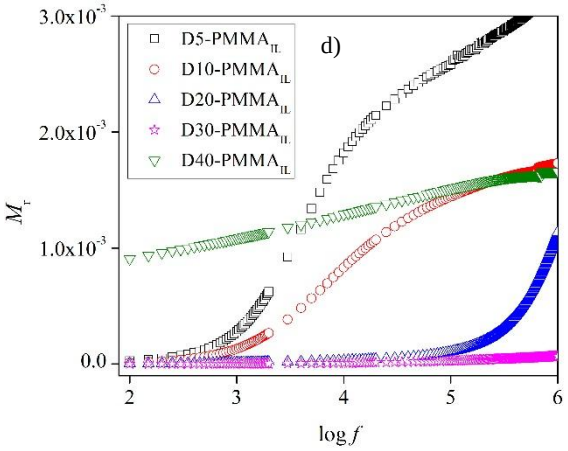

Fig. 5: (a) ε_r vs. log f, (b) ε_i vs. log f, (c) M_r vs. log f and (d) M_i vs. log f for Dx-$PMMA_{IL}$ at 303 K

IV. CONCLUSION

Solid, flexible, transparent and free standing films were successfully obtained with the addition of <50 wt % LiTf into the $PMMA_{IL}$ matrix. The FTIR analyses confirmed that the interaction had occurred between the two potential coordinating sites of PMMA and the lithium cation of the salt via dative bond. The highest ionic conductivity achieved was 2.65 $\times 10^{-4}$ S cm^{-1} with the incorporation of 30 wt% of LiTf. This is due to the suppression of the semicrystalline structure of $PMMA_{IL}$ that lead to the formation of more amorphous phase which contribute to the highest value of n, μ and D of free ions of the sample.

ACKNOWLEDGMENT

The authors would like to express their gratitude to the Faculty of Applied Sciences, UiTM, i-MADE Lab and Institute of Science for their support in providing research facilities to carry out this research. Financial support from Malaysia Toray Science Foundation (MTSF) (Ref: TMLC-CA/13.206 [File Ref: 16/G236]), Bestari Perdana grant (Ref. No: 600-IRMI/PERDANA 5/3 BESTARI (083/2018)) and MyBrain SC scholarship are highly acknowledged.

REFERENCES

1. Rajendran, S., Sivakumar, M., & Subadevi, R. (2004). Investigations on the effect of various plasticizers in PVA–PMMA solid polymer blend electrolytes. *Materials Letters*, 58(5), 641-649.
2. Chew, K. W., & Tan, K. W. (2011). The effects of ceramic fillers on PMMA-based polymer electrolyte salted with lithium triflate, $LiCF_3SO_3$. *International Journal of Electrochemical Science*, 6, 5792-5801.
3. Latif, F.A. (2006). *Preparation and characterization of poly (methyl methacrylate)/50% epoxidised natural rubber based solid electrolytes for lithium-ion secondary battery* (Doctoral dissertation, Universiti Teknologi Malaysia).
4. Xie, Z. L., Xu, H. B., Geßner, A., Kumke, M. U., Priebe, M., Fromm, K. M., & Taubert, A. (2012). A Transparent, flexible, ion conductive, and luminescent PMMA ionogel based on a Pt/Eu bimetallic complex and the ionic liquid [Bmim][$N(Tf)_2$]. *Journal of Materials Chemistry*, 22(16), 8110-8116.

5. Xie, Z. L., Jeličić, A., Wang, F. P., Rabu, P., Friedrich, A., Beuermann, S., & Taubert, A. (2010). Transparent, flexible, and paramagnetic ionogels based on PMMA and the iron-based ionic liquid 1-butyl-3-methylimidazolium tetrachloroferrate (III) [Bmim][$FeCl_4$]. *Journal of Materials Chemistry*, 20(42), 9543-9549.
6. Agrawal, R. C., & Pandey, G. P. (2008). Solid polymer electrolytes: materials designing and all-solid-state battery applications: An overview. *Journal of Physics D: Applied Physics*, 41(22), 223001.
7. Zailani, N. A. M., Latif, F. A., Ali, A. M. M., Zainuddin, L. W., Kamaruddin, R., & Yahya, M. Z. A. (2017). Effect of ionic liquid incarceration during free radical polymerization of PMMA on its structural and electrical properties. *Ionics*, 23(2), 295-301.
8. Azuan, M., Husna, S. I., Abdul Latif, F., Zamri, M., & Fadli, S. (2016). Effects of dodecanoic acid modified SiO_2 on filler dispersion and ionic conductivity of PMMA/ENR-50/$LIBF_4$ electrolytes. *Materials Science Forum*, 846, 528-533.
9. Shukla, N., & Thakur, A. K. (2009). Role of salt concentration on conductivity optimization and structural phase separation in a solid polymer electrolyte based on PMMA-$LiClO_4$. *Ionics*, 15(3), 357–367.
10. Muhammad, F. H., Jamal, A., & Winie, T. (2016). Dielectric and AC conductivity behavior of hexanoyl chitosan-NaI based polymer electrolytes. *International Journal of Advanced and Applied Sciences*, 3(10), 9-13.
11. Pavia, D. L., Lampman, G. M., Kriz, G. S., & Vyvyan, J. A., *Introduction to spectroscopy*, Cengage Learning, (2008).
12. Sim, L. N., Majid, S. R., Arof, A. K. (2012). FTIR studies of PEMA/PVdF-HFP blend polymer electrolyte system incorporated with $LiCF_3SO_3$ salt. *Vibrational Spectroscopy*, 58, 57-66.
13. Jamal, A., Muhammad, F. H., Ali, A. M. M., & Winie, T. (2017). Blends of hexanoyl chitosan/epoxidized natural rubber doped with EMImTFSI. *Ionics*, 23(2), 357-366.
14. Chowdari, B. V. R., Gopalakrishnan, R., & Tan, K. L. (1990). ESCA studies of fast ion conducting glasses. *Solid State Ionics*, 40, 709-713.
15. Deraman, S. K., Mohamed, N. S., & Subban, R. H. Y. (2014). Ionic liquid incorporated PVC based polymer electrolytes: electrical and dielectric properties. *Sains Malaysiana*, 43(6), 877-883.
16. Abidin, S. Z. Z., Yahya, M. Z. A., Hassan, O. H., & Ali, A. M. M. (2014). Conduction mechanism of lithium bis(oxalato) borate–cellulose acetate polymer gel electrolytes. *Ionics*, (2012), 1671-1680.

AUTHORS PROFILE

Nabilah Akemal Muhd Zailani (PhD) received her PhD from Universiti Teknologi MARA Shah Alam in 2019. Her research interest includes synthesis of a new polymer electrolyte for application in supercapacitors.

Famiza Abdul Latif (PhD) is an Associate Professor in Faculty of Applied Sciences at Universiti Teknologi MARA Shah Alam. She received her PhD from Universiti Teknologi Malaysia in 2006. Her research interest includes synthesis of a solid polymer electrolyte and liquid polymer electrolytes for application in energy storage devices.

Abdul Malik Marwan Ali (PhD) is an Associate Professor in Faculty of Applied Sciences at Universiti Teknologi MARA Shah Alam. He received his PhD from UiTM Shah Alam in 2008. His research interest include solid state ionics, polymer electrolytes, lithium ion battery, supercapacitors, solar cells and first principles computational studies.

Mohd Azri Ab Rani (PhD) is a senior lecturer in Faculty of Applied Sciences at Universiti Teknologi MARA Shah Alam. He received his PhD from Imperial College London in 2012. His research interest includes synthesis of ionic liquid.

Muhd Zu Azhan Yahya (PhD) is a Professor in Faculty of Defence Science & Technology at Universiti Pertahanan Nasional Malaysia. He received his PhD from Universiti Malaya in 2002. His research interest include solid state ionics, polymer electrolytes, lithium ion battery, supercapacitors, solar cells and first principles computational studies.